Pacific Graphics (2014)
J. Keyser, Y. J. Kim, and P. Wonka (Editors)

Short Paper

Surface mesh segmentation and reconstruction with smooth boundary curves

Shoichi Tsuchie[1] and Masatake Higashi[2]

[1]Nihon Unisys, Ltd., Japan
[2]Toyota Technological Institute, Japan

Abstract

In mesh segmentation for industrial design objects, each segment defined by a region with closed boundary should correspond to its underlying surface constructed according to the designer's intention. In order to generate those segments from the scanned data, we propose a method in which (i) more suitable regions are extracted by the region splitting/merging processing with a new splitting scheme from the obtained clusters, (ii) smooth and consistent boundaries are generated as intersection or contacting curves between the adjacent underlying surfaces, and (iii) the region is reconstructed with high-quality triangle facets. We demonstrate the effectiveness of our method by applying it to the scanned data of the real-world industrial design objects.

Categories and Subject Descriptors (according to ACM CCS): I.4.6 [Computer Graphics]: Segmentation—Region growing, partitioning

1. Introduction

Segmentation has been an important research item in area such as image processing and object tracking, besides geometry processing. This paper focuses on the surface-type segmentation [Sha08] for the scanned data of the industrial design objects. In automobile styling design, designers generate a *surface-model* by constructing base surfaces, approach surfaces and fillets step by step [HKN83]. Each surface is equivalent to what clay modelers can scrape off the clay by sweeping one curve rule [Yam93]. On the other hand, in reverse-engineering, we have to extract the *segments*, each of which is defined by a region with closed boundary, from scanned data corresponding to the underlying (more precisely trimmed) surfaces of *surface-model*. The *segment* should satisfy the following requirements:

(i) More suitable regions should be extracted according to the designer's intention. We have to divide the data corresponding to a subtle change of curvature. Furthermore, we have to split the area where is smoothly connected with G^2 condition in such a case as shown in Fig. 1.

(ii) Smooth and consistent boundaries should be generated against noise and deficiency of the data. Consistent boundaries define a curve network in which each cell defines one region by closed boundary loop. The sharp edges are represented by the intersection curves between the adjacent underlying surfaces, because they cannot be represented by a single smooth surface and often become blunt due to both measurement error and geometry processing.

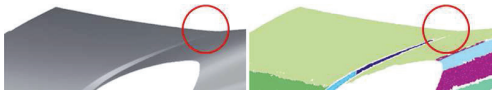

Figure 1: *Smoothly connected area and its segmentation: the segmentation was conducted using the method [THH14].*

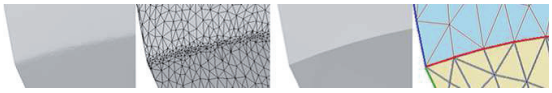

(a) Scanned mesh (b) Our result

Figure 2: *Mesh around edge and the obtained segments.*

This paper addresses the issue of generating the high-quality *segments* satisfying (i) and (ii), and the mesh reconstruction scheme which satisfies the following condition:

(iii) High-quality triangle facets defined by almost equilateral triangles within a specified tolerance from the original data are used for representing the regions.

Fig. 2 shows an example of our results in which the smooth boundaries are obtained as sharp edges and the regions are reconstructed with high-quality triangle facets in Fig. 2 (b).

DOI: 10.2312/pgs.20141247

1.1. Related work

In this subsection, we review some representative methods with respect to the above requirements.

(i) Region extraction: the methods based on the quadric surface fitting were widely studied in many papers and demonstrated the effectiveness to the data of mechanical part including noise, but the following problems were pointed out: the extracted regions heavily depended on the tolerance of surface fitting [VHB08], and the use of only quadric surface was not flexible to identify complicated models [YWLY12]. Therefore, it is difficult to apply the methods to the industrial design data including measurement error, because the quadric surface is not adequate for detecting a subtle change of curvature in the design objects.

There exist only a few studies as [VS05] and [THH14] which applied their methods to design objects. First, [VS05] used bicubic Bézier surface fitting. In this method, each region compatible with Bézier surface was extracted through the *region growing* method from a seed instead of the splitting/merging operations. Therefore, in such an area connected in G^2 as shown in Fig. 1, we cannot predict where the area is divided or whether it is done, and the method heavily depends on the initial seeds which are generated by contracting the regions in a morphological manner.

Second, the method proposed in [THH14] generated the clustered vertices according to the curvature values based on a clustering technique robust to noise, and was developed for the segmentation of the industrial design objects. Different from the method using the *k-means* (Lloyd) clustering algorithm in [LDB04a] etc., [THH14] did not suffer from the over-segmentation problem, but this method cannot split the G^2 connected area (Fig. 1) in principle, because there is no change of curvature value in such area.

(ii) Boundary generation: [VS05] insisted that the boundaries were represented by the intersections of the underlying surfaces themselves although the implementation and evaluation had not been performed. This approach satisfies the requirement (ii), but there is the following problem: the underlying surfaces used for region extraction were usually created for each region without any G^1/G^2 boundary condition. Therefore, it is difficult to deal with the contact calculation by them to generate smooth curves.

A lot of methods such as *graph-cut* [YSOM10, YWLY12], *geometric snake (active contour)* [LL02, JK04, KT09] and contour tracking in the minimum direction of principal curvatures [LDB04b] were proposed in order to smooth or rectify the zigzag boundaries as post-processing of mesh segmentation. But these methods cannot directly satisfy the requirement (ii) since the curves were defined on the data including noise; sharp edges are represented by the curves on the blunt data instead of the intersection curves.

In the image segmentation, the *region competition* method [ZY96] was proposed. This method provided the mechanism

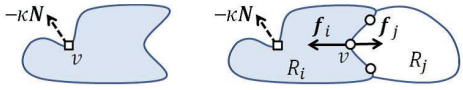

(a) Snake (Active contour) (b) Region competition

Figure 3: *Region competition.*

that the boundary smoothing was performed by the curvature smoothing flow (Fig. 3 (a)) under a constraint between the boundary and its adjacent regions (Fig. 3 (b)). The constraint is defined as a force $\boldsymbol{f}_i$ which prevents amount of characteristic such as the averaged intensity, etc. defined on each region R_i from changing drastically by the boundary movement. Compared with the geometric snake model in which the motion of boundary curve is constrained on a single surface, sufficient studies of the *region competition* framework have not been conducted in mesh segmentation. Hence, applying the idea of this framework to the mesh segmentation, we develop a method of generating segment boundaries.

1.2. Contributions

The main ideas behind our approach for tackling the issues in the existing methods with respect to (i) and (ii) are composed of the following two items:

- a curvature-based clustering method accompanied by the splitting/merging framework to which a new region splitting scheme is added,
- to generate the smooth and consistent boundaries compatible with the adjacent underlying surfaces.

First, in order to extract more suitable regions, we adopt the clustering method [THH14], and conduct the region splitting/merging processing by checking the compatibility of a surface fitting. The issue how to specify the optimum number of clusters M in the clustering approach can be settled by the splitting/merging processing. But in the combination of the existing techniques, we cannot tackle the problem of splitting the G^2 connected area as shown in Fig. 1 which is a special case but is often occurs in styling design data. Hence, we develop a new splitting scheme based on the morphological processing which make a region extend (dilation) or contract (erosion).

In the existing geometry processing, the morphological operations is used to extract feature lines (skeletonizing) in [RKS00] and used to generate seeds in [VS05] mentioned above. Now, we focus on the above problem: the shape of boundaries are complicated by being cut with design reliefs and character-lines. Meanwhile, morphological operation is applied to not region but boundary. Thus, the morphological operations may become a means to split the region with the characteristic boundary.

Second, applying the idea of *region competition* method [ZY96], we introduce a boundary smoothing equation constrained on the fitted surfaces of the adjacent regions. The region force $\boldsymbol{f}_i$ (Fig. 3 (b)) is defined by the deviation between boundary curve and each fitted surface. Hence, a point on

the curve converges to the minimum point from the surfaces during the smoothing process which is done similarly in the usual process. By this calculation, the point converges on the intersection curve of the surfaces for G^0 boundary point, and that on the line through two points of giving the shortest distance between surfaces with common surface normal vector for G^1/G^2 boundary.

The rest of this paper is organized as follows: Sec. 2 presents the whole procedure of our segmentation. We explain our proposal methods in Sec. 3 and show experimental results in Sec. 4. Finally, we conclude the paper in Sec. 5.

2. Procedure of our segment generation

In this section, we describe the whole procedure of our segment generation, which is composed of three parts:

1. Initial segmentation (Step1 to 3): we obtain the regions which are disjoint each other via the method [THH14].
2. Region extraction (Step4 to 8): we extract the connected regions compatible with the underlying surfaces, and obtain the boundaries which are zigzag curves but topologically consistent.
3. *Segment* generation (Step9): we generate the smooth and consistent boundaries compatible with the adjacent underlying surfaces by the *region competition* method, and reconstruct meshes with high-quality triangles.

Step1) Vertex clustering: conducting the vertex clustering with a specified number of clusters M, we obtain the the labeled vertices with the integer m $(1 \leq m \leq M)$ according to the change of curvatures (Fig. 4(c)).
Step2) Feature vertex extraction: we extract the feature vertices defined near on sharp edges and fillet edges.
Step3) Base-region extraction: we extract the meshes connecting the same labeled vertices excluding the one obtained in Step2, and call each mesh *base-region* (Fig. 4 (d)).
Step4) Morphological region splitting: we further divide the base-region using the *morphological region splitting* method described in Sec. 3.1.
Step5) Surface fitting & region splitting: for each base-region, we conduct a surface fitting. As opposed to the region whose fitting surface does not satisfy the specified tolerance, we repeat the following steps: Step1 with the condition M=2 and Step3 until the tolerance for each region is satisfied.
Step6) Crack filling: to fill the cracks between regions which are generated by the feature vertices removal in Step3, we expand each region to which we add its adjacent facets in the cracks.
Step7) Boundary extraction & topology construction: we extract the outer boundary for each region, and construct the segment topology combining the obtained boundaries.
Step8) Region merging: for the adjacent regions R_1 and R_2 which share the common boundary, we merge R_1 into R_2 if R_1 is represented by the underlying surface of R_2 within the tolerance (Fig. 4 (g)).

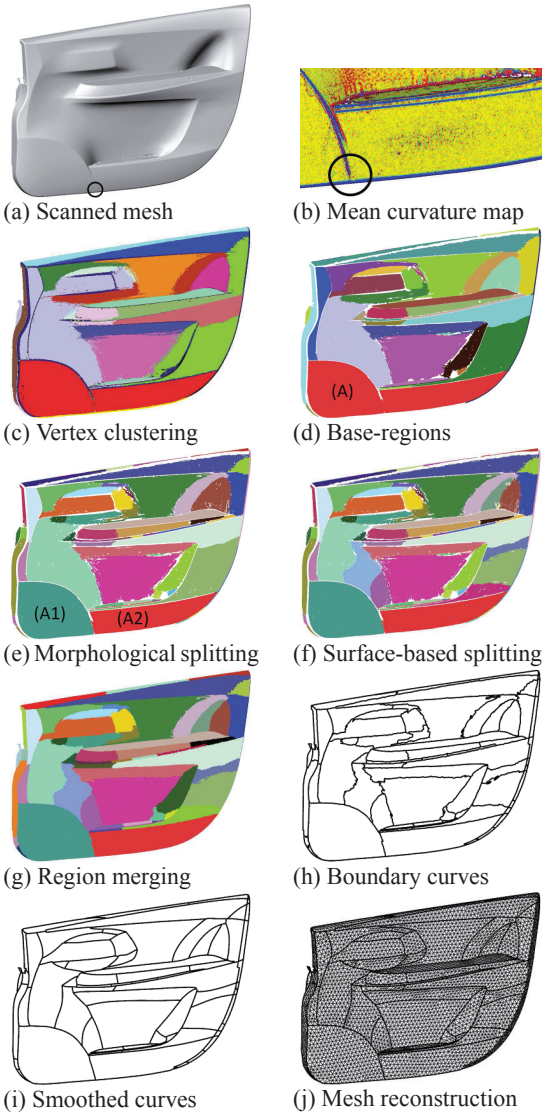

(a) Scanned mesh (b) Mean curvature map
(c) Vertex clustering (d) Base-regions
(e) Morphological splitting (f) Surface-based splitting
(g) Region merging (h) Boundary curves
(i) Smoothed curves (j) Mesh reconstruction

Figure 4: *Procedure of segment generation (our result).*

Step9) Segment generation: we smooth the zigzag boundary curves (Fig. 4 (h), (i)), and then reconstruct the region meshes of high-quality triangle facets as shown in Fig. 4 (j). The details are described in Sec. 3.2 and Sec. 3.3.

3. Our methods

First, we propose a method called *morphological region splitting* in Sec. 3.1. Next, we explain our boundary calculation in Sec. 3.2 and mesh reconstruction scheme in Sec. 3.3.

3.1. Morphological region splitting

For each base-region R_0 (Fig. 5 (a)), we contract R_0 by removing the facets connecting to the boundary of R_0 until it is split into several regions $\{R_i\}(i=1,2,\cdots)$ s.t. $\cup_{i=1} R_i \subset R_0$

as shown in Fig. 5 (b). If R_0 and $\{R_i\}$ satisfy the following criteria, then we expand each region R_i until $\cup_{i=1} R_i = R_0$ (Fig. 5 (c)). These operations are recursively conducted.

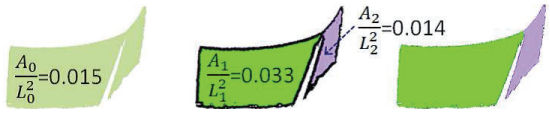

(a) Base-region (b) Contraction (c) Expansion

Figure 5: *Morphological region splitting.*

Criteria: Assume that $\{R_i\}$ are sorted in descending order with respect to the number of vertices $|R_i|$. Then,

$$\text{(i) } |R_0| > T_{min}, \quad \text{(ii) } \frac{|R_1|}{|R_0|} > \varepsilon_1, \quad \text{(iii) } \frac{A_1}{L_1^2} \geq \frac{A_0}{L_0^2}. \tag{1}$$

(i) and (ii) mean that we do not apply the morphological split to a small region. (iii) prevents from generating new narrower region R_1 than R_0, because the ratio of area and squared length of the region $\frac{A}{L^2}$ has a small value for thin region. For 2D case, the following inequality called *isoperimetric inequality* is satisfied: $\frac{4\pi A}{L^2} \leq 1$.

3.2. Segment boundary calculation

Region competition method in the image segmentation is formulated by the evolution equation of any point $\boldsymbol{v}$ in the pixel coordinate (u,v). The equation of $\boldsymbol{v}(u,v)$ on the common boundary of regions R_i and R_j is given by

$$\frac{d}{dt}\boldsymbol{v}(u,v;t) = \underbrace{-\kappa_{v(i)}\boldsymbol{N}_{v(i)}}_{Smoothing} + \underbrace{\log P(I_v|\alpha_i))\boldsymbol{N}_{v(i)} + \log P(I_v|\alpha_j))\boldsymbol{N}_{v(j)}}_{Region\ competition}, \tag{2}$$

where $\kappa_{v(i)}$ and $\boldsymbol{N}_{v(i)}$ are the curvature and outward normal vector at $\boldsymbol{v}$ from the side of R_i, respectively. $P(I_i|\alpha_i)$ is the likelihood of the intensity I in the region R_i with the parameter α_i. Here, $\boldsymbol{f}_i \equiv \log P(I_v|\alpha_i)\boldsymbol{N}_{v(i)}$ is called the *statistics force* and this always compresses the region, since $\log P \leq 0$. In addition, since $\boldsymbol{N}_{v(i)} = -\boldsymbol{N}_{v(j)}$ on the common boundary, this relation describes the situation in Fig. 3 (b). Applying the above idea to our segment boundary calculation, we develop an equation to generate smooth boundary curves below.

We let the competition forces be the ones which control deviation from the regions, and formulate it as follows:

- true boundary point $\boldsymbol{x}^*$ exists on the underlying surfaces,
- the deviation between $\boldsymbol{x}^*$ and the point $\boldsymbol{v}$ on scanned data is pulled back by the spring force, $\boldsymbol{f} = -k(\boldsymbol{v} - \boldsymbol{x}^*)$, to the underlying surfaces.

Thus, the region competition terms are defined as follows:

$$-k_{R_i}(\boldsymbol{v} - \boldsymbol{x}^*_{R_i}) - k_{R_j}(\boldsymbol{v} - \boldsymbol{x}^*_{R_j}), \tag{3}$$

where k_{R_i} is the spring constant for the region R_i.

Next, the smoothing term in Eq. (2) is an example of the typical curvature smoothing flow accompanying area shrinking. Hence, we use the averaged curvature flow proposed in [HPP05] which is area preserving. In its space curve formalization, let $\boldsymbol{T}$, $\boldsymbol{N}_1$ and $\boldsymbol{N}_2$ be an orthogonal rotation minimization frame along a curve with tangent vector $\boldsymbol{T}$. The curvature vector $\boldsymbol{\kappa}_v$ at point $\boldsymbol{v}$ on the curve can be decomposed as $\boldsymbol{\kappa}_v = \kappa_{v,1}\boldsymbol{N}_{v,1} + \kappa_{v,2}\boldsymbol{N}_{v,2}$. Thus, the equation of space curve smoothing was given by

$$\frac{d}{dt}\boldsymbol{v}(x,y,z;t) = (\kappa_{v,1} - \kappa^{(s)}_{v,1})\boldsymbol{N}_{v,1} + (\kappa_{v,2} - \kappa^{(s)}_{v,2})\boldsymbol{N}_{v,2}, \tag{4}$$

where $\kappa^{(s)}_{v,i} \equiv \kappa_{v,i} - \Delta\kappa_{v,i} (i = 1,2)$ and Δ denotes the Laplacian operator.

From the above preparation, our proposed equation is described by combining Eq. (3) and Eq. (4) as follows:

$$\begin{aligned}\frac{d}{dt}\boldsymbol{v}(x,y,z;t) =& (\kappa_{v,1} - \kappa^{(s)}_{v,1})\boldsymbol{N}_{v,1} + (\kappa_{v,2} - \kappa^{(s)}_{v,2})\boldsymbol{N}_{v,2} \\ &+ k_{R_i}(\boldsymbol{x}^*_{R_i} - \boldsymbol{v}) + k_{R_j}(\boldsymbol{x}^*_{R_j} - \boldsymbol{v}).\end{aligned} \tag{5}$$

Convergent condition: for any point $\boldsymbol{v}^t$ on common boundary in the t-th step and a given threshold value ε_2,

$$\|\boldsymbol{v}^{t+1} - \boldsymbol{v}^t\| \leq \varepsilon_2. \tag{6}$$

Here, we assume that the point $\boldsymbol{x}^*_{R_i}$ exists near the point $\boldsymbol{v}$, and set $\boldsymbol{x}^*_{R_i}$ as the nearest point on the underlying surface of R_i from $\boldsymbol{v}$. Then, Eq. (5) describes that the point $\boldsymbol{v}$ converges to the minimum distant point between two underlying surfaces during the evolution process. Fig. 6 and Fig. 7 indicate the situations for G^0 and G^1/G^2 boundary, respectively.

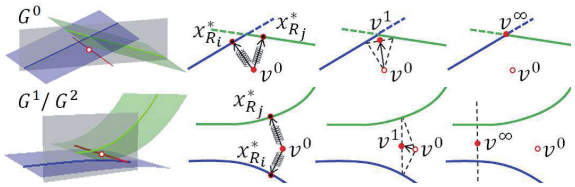

Figure 6: *Type of boundary: G^0 (upper) and G^1/G^2 (lower).*

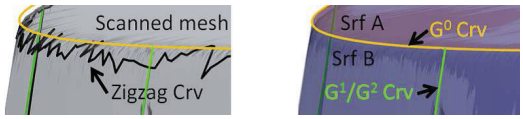

Figure 7: *Example of segment boundaries (our result).*

3.3. Reconstruction of segment region

We reconstruct the mesh for each segment by using the obtained smooth curves in Sec. 3.2 and the fitted surfaces. The procedure is as follows: let (u,v,w) be the local coordinate defined in the surface fitting for each base-region. Then,

1. Divide the boundary network curves with a specified length (Fig. 8 (a)), and then project them onto the plane $w=0$ in which equilateral triangles are covered.
2. Extract triangles inside the boundary curves (Fig. 8 (b)).
3. Fill cracks between boundary and the extracted triangles in step 2 (Fig. 8 (c)).

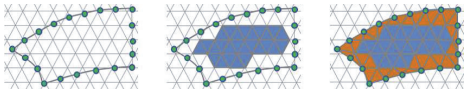

(a) Boundary (b) Inner mesh (c) Crack

Figure 8: *Reconstruction of segment region.*

4. Project triangles onto the underlying surface and transform into the real space(x,y,z).

After the above step 3, we relax distortion of the triangle near the boundary using the processing which restrains boundary vertices and moves internal ones by the Laplacian scheme with the weight $w_\lambda=(l^2_{\lambda,1}+l^2_{\lambda,2}+l^2_{\lambda,3})/A_\lambda$. Here, A_λ is the area of λ-th triangle connecting to the vertex V_i and $l_{\lambda,j}$ is the side length. Note that $Q(\triangle_\lambda)\equiv 4\sqrt{3}/w_\lambda$ is known as a triangle quality measure proposed in [Lo89], and has the value between 0 (degenerate) and 1 (equilateral triangle).

4. Results

We have implemented our proposed method using MS VC++2013 on the desktop Intel/i7® 4771 (3.5GHz, 4 core) computer. To demonstrate the effectiveness of our method, we conducted some experiments for three data which are all real-world scanned data of automobile style-design objects. In all experiments, we used the following conditions:

- the number of cluster M=20 in Step1 of our segmentation procedure described in Sec. 2,
- the tolerance of surface fitting are set as follows: more than 90% of vertices of each base-region mesh are in less than ±0.2mm of distance from each fitting surface,
- T_{min}=0.05% of the whole facets in the data, ε_1=0.25 in Eq. (1), $k_{R_i}=k_{R_j}=0.5$ in Eq. (5), and ε_2=0.001 in Eq. (6),
- reconstructed mesh size is 15mm.

First, Fig. 4 shows the results for a typical part of car interior. We can observe the following two facts from the figure:

- the region marked (A) in Fig. 4 (d) was split into two regions (A1) and (A2) in Fig. 4 (e) by the morphological region splitting,
- for the zigzag boundaries in Fig. 4 (h) obtained after region merging processing, our proposed Eq. (5) generated the smooth segment boundaries shown in Fig. 4 (i), and high-quality triangle mesh was obtained in Fig. 4 (j).

For the second point, Fig. 7 shows the enlarged part in Fig. 4 (j). Although the zigzag curves are on the scanned data, the obtained smooth curves are represented by the intersections between the adjacent fitted surfaces. Fig. 9 shows the similar results as well as those in Fig. 4.

Next, Fig. 10 and Fig. 11 show the results for a car exterior, from which we can observe the above same facts:

- the morphological splitting worked effectively. (A), (B) and (C) marked in Fig. 10 (a) were split into (A1)/(A2), (B1)/(B2) and (C1)/(C2)/(C3), respectively in Fig. 10 (b),
- the obtained segments in Fig. 10 (c), (d) nearly correspond to the areas surrounded by the character-lines in Fig. 10 (e) which designers created,

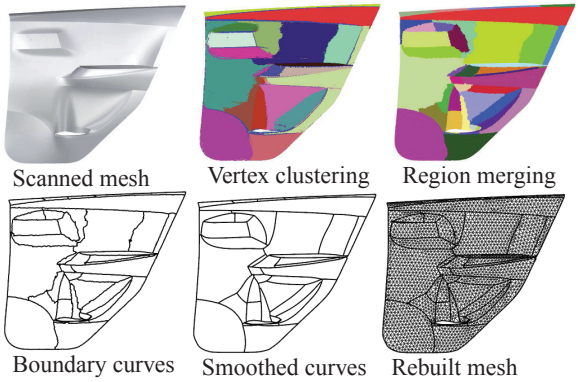

Figure 9: *Result for door trim (rear part)*

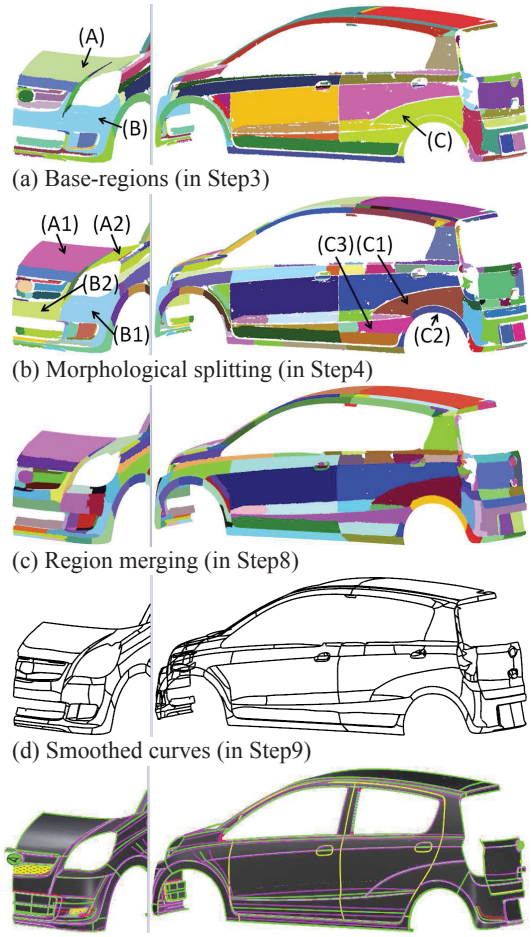

(a) Base-regions (in Step3)

(b) Morphological splitting (in Step4)

(c) Region merging (in Step8)

(d) Smoothed curves (in Step9)

(e) Character-lines of CAD data

Figure 10: *Result for the scanned data of a car in the market. Enlarged figure of (A) is shown in Fig. 1 and Fig. 5.*

- the consistent smooth boundaries and high-quality mesh in Fig. 11 were generated.

Table 1 lists the model size, the number of regions after each step described in Sec. 2, and the runtime performance.

Table 1: *Size of the scanned data (In) and reconstructed mesh (Out), the number of regions after each processing, and total processing time. B-R denotes the base-regions which are generated in Step3 described in Sec. 2. Split1 and Split2 denote the morphological splitting in Step4 and surface fitting based splitting in Step5, respectively.*

Model (L[mm]×W[mm]×H[mm])	In (facets)	Out (facets)	B-R	Split1	Split2	Merge	Elaps [min]
Fig. 4 Door trim/Fr (949×105×668)	1,721,517	6,894	40	68	74	58	35
Fig. 9 Door trim/Rr (793×81×687)	1,094,624	4,571	29	63	72	44	26
Fig. 10 Car exterior (3395×923×1308)	2,164,666	46,026	94	145	176	145	59

(a) Scanned (left) and reconstructed (right) mesh

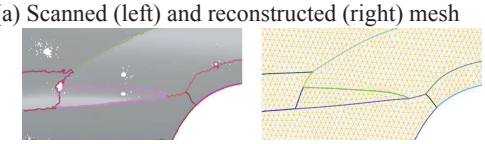

(b) Zigzag (left) and smooth (right) curves

Figure 11: *Reconstructed segments*

A limitation of our study is that the presented method is unsuitable for application to the objects such as organic ones, because our study focuses on the industrial design objects which are constructed by the underlying surfaces with monotonically varying curvature.

5. Conclusions

We have presented a method of surface mesh segmentation and its reconstruction for the scanned data of the industrial design objects. Through the experiments using real-world scanned data, we have obtained the following conclusion:

- a curvature-based clustering method accompanied by the splitting/merging framework to which a new region splitting scheme is added can extract more suitable regions according to the designer's intention,
- our proposed method can generate the smooth and consistent boundaries compatible with those intersected by the adjacent underlying surfaces both in G^0 and G^1/G^2, and reconstruct the regions with high-quality triangle facets.

Although we have generated high-quality mesh structure for the segment, for representing it with the surfaces, we have to cancel the gap shown in the lower figure of Fig. 6 and strictly connect in the G^1/G^2 boundaries. Future research includes the surface fitting under the boundary conditions.

Acknowledgment

We would like to appreciate that Daihatsu Motor Co., Ltd. provided the real-world data shown in this paper.

References

[HKN83] HIGASHI M., KOHZEN I., NAGASAKA J.: An interactive cad system for construction of shapes with high-quality surface. *Computer Applications in Production and Engineering North-Holland* (1983), 371–390.

[HPP05] HILDEBRANDT K., POLTHIER K., PREUSS E.: Evolution of 3d curves under strict spatial constraints. *Ninth International Conference on Computer Aided Design and Computer Graphics (CAD/CG 2005)* (2005), 40–45.

[JK04] JUNG M., KIM H.: Snaking across 3d meshes. *PG '04: Proceedings of the 12th Pacific Conference on Computer Graphics and Applications* (2004), 87–93.

[KT09] KAPLANSKY L., TAL A.: Mesh segmentation refinement. *Computer Graphics Forum 28*, 7 (2009), 1995–2003.

[LDB04a] LAVOUÉ G., DUPONT F., BASKURT A.: Constant curvature region decomposition of 3d-meshes by a mixed approach vertex-triangle. *Journal of WSCG 12*, 2 (2004), 245–252.

[LDB04b] LAVOUÉ G., DUPONT F., BASKURT A.: Curvature tensor based triangle mesh segmentation with boundary rectification. *CGI '04: Proceedings of the Computer Graphics International* (2004), 10–17.

[LL02] LEE Y., LEE S.: Geometric snakes for triangular meshes. *Computer Graphics Forum 21*, 3 (2002), 229–238.

[Lo89] LO S. H.: Generating quadrilateral elements on plane and over curved surfaces. *Computer and Structures 31*, 3 (1989), 421–426.

[RKS00] RÖSSL C., KOBBELT L., SEIDEL H.-P.: Extraction of feature lines on triangulated surfaces using morphological operators. *In: Smart Graphics, Proceedings of the 2000 AAAI Symposium* (2000), 71–75.

[Sha08] SHAMIR A.: A survey on mesh segmentation techniques. *Computer Graphics Forum 27*, 6 (2008), 1539–1556.

[THH14] TSUCHIE S., HOSINO T., HIGASHI M.: High-quality vertex clustering for surface mesh segmentation using student-t mixture model. *Computer-Aided Design 46* (2014), 69–78.

[VHB08] VANČO M., HAMANN B., BRUNNETT G.: Surface reconstruction from unorganized point data with quadrics. *Computer Graphics Forum 27*, 6 (2008), 1593–1606.

[VS05] VIEIRA M., SHIMADA K.: Surface mesh segmentation and smooth surface extraction through region growing. *Computer Aided Geometric Design 22*, 8 (2005), 771–792.

[Yam93] YAMADA Y.: *Clay Modeling: Techniques For Giving Three-Dimensional Form To Idea*. Sanéishobo Publishing, 1993.

[YSOM10] YANG C., SUZUKI H., OHTAKE Y., MICHIKAWA T.: Mesh segmentation refinement. *International Journal of CAD/CAM 10*, 1 (2010), 11–19.

[YWLY12] YAN D.-M., WANG W., LIU Y., YANG Z.: Variational mesh segmentation via quadric surface fitting. *Computer-Aided Design 44* (2012), 1072–1082.

[ZY96] ZHU S. C., YUILLE A.: Region competition: Unifying snakes, region growing, and bayes/mdl for multiband image segmentation. *IEEE Transaction on Pattern Analysis and Machine Intelligence 18*, 9 (1996), 884–900.